Histol Histopathol (2025) 40: 1239-1251

Histology and Histopathology
From Cell Biology to Tissue Engineering

ORIGINAL ARTICLE Open Access

Hsa_circ_0088036 promotes tumorigenesis and chemotherapy resistance in hepatocellular carcinoma via the miR-140-3p/KIF2A axis

Zhong Wang[1], Lei Wang[2], Guoqing Yin[1], Heng Li[3], Rong Zhang[3], Yuan Feng[1] and Wen Chang[4]

[1]Department of Oncology, [2]Department of Pathology, [3]Department of Gastroenterology and [4]Department of Pharmaceutical, Yan'an University Xianyang Hospital, Xianyang City, Shaanxi Province, PR China

Summary. Background. Hepatocellular carcinoma (HCC) is a cancer with high morbidity and mortality. There are limited treatment options, particularly for chemotherapy-resistant HCC patients. Circular RNA hsa_circ_0088036 was associated with the development of bladder cancer and non-small cell lung cancer. However, whether it might be a potential therapeutic target for HCC remains elusive.

Methods. Hsa_circ_0088036 expression was detected in HCC tumor tissues and cell lines using real-time PCR. The influences of hsa_circ_0088036 on proliferation and invasion as well as chemotherapy sensitivity in HCC cells were investigated by gain- and loss-of-function analyses. Associations among hsa_circ_0088036, miR-140-3p, and KIF2A were validated by real-time PCR, miRNA pull-down assay, dual-luciferase reporter assay, and western blot. Furthermore, a rescue experiment using KIF2A overexpression was performed to evaluate the regulatory mechanism of hsa_circ_0088036 in HCC cells. Additionally, the effect and mechanism of hsa_circ_0088036 were confirmed in a xenograft mouse model.

Results. Hsa_circ_0088036 was highly expressed in HCC tissues and cells, with even higher expression in oxaliplatin-resistant cells. This expression was positively correlated with tumor size and TNM stage of the patients. Overexpression of hsa_circ_0088036 promoted the proliferation and invasion of HCC cells, while silencing mediated the opposite effects. Meanwhile, knockdown of hsa_circ_0088036 enhanced chemotherapy sensitivity, including oxaliplatin, doxorubicin, and sorafenib, in HCC cells. Furthermore, hsa_circ_0088036 silencing inhibited tumor growth and increased oxaliplatin sensitivity *in vivo*. Mechanically, hsa_circ_0088036 functioned via the miR-140-3p/KIF2A axis with the activation of PI3K/Akt and Notch signaling pathways.

Conclusions. Hsa_circ_0088036 promoted HCC tumorigenesis and chemotherapy resistance by activating the PI3K/Akt and Notch pathways through regulating miR-140-3p/KIF2A signaling. Thus, hsa_circ_0088036 may be a potential therapeutic target in chemotherapy-resistant HCC.

Key words: Hsa_circ_0088036, Hepatocellular carcinoma, Oxaliplatin resistance, miR-140-3p, KIF2A

Introduction

Liver cancer is the sixth most common cancer and the third leading cause of cancer death worldwide with approximately 960,000 new cases and 830,000 deaths per year (Sung et al., 2021). Hepatocellular carcinoma (HCC) is the most common form of liver cancer, with limited treatment options; the five-year relative survival rate is only about 18% (Llovet et al., 2021; Hou et al., 2022; Vogel et al., 2022). Oxaliplatin is effective for the treatment of HCC, however, primary or acquired resistance to oxaliplatin is still a major challenge in clinical practice (Shi et al., 2023). Therefore, the identification of the mechanisms of tumorigenesis and oxaliplatin resistance in HCC is urgently needed.

Circular RNAs (circRNAs) are single-stranded, covalently closed noncoding RNAs generated from linear precursor mRNA by reverse splicing events (Xue et al., 2022). They are more stable than linear RNAs and cannot be degraded by RNA exonuclease because of the lack of 5'-3' polarity and a polyadenylated tail (Zhu et al., 2021; Xue et al., 2022). They are associated with

Corresponding Author: Wen Chang, Pharmaceutical Department, Yan'an University Xianyang Hospital, No. 38 Wenlin Road, Xianyang City 712000, Shaanxi Province, China. e-mail: changwen_c@126.com
www.hh.um.es. DOI: 10.14670/HH-18-849

several human pathological and physiological processes. Accumulating evidence indicates that circRNAs can regulate gene expression by sponging miRNAs (Huang et al., 2020; Yu et al., 2023). CircRNAs are aberrantly expressed and participate in the progression of various cancers, including HCC (Lin et al., 2022; Meng et al., 2023; Shen et al., 2023). For example, circRanGAP1 was enhanced in HCC cells and tumor tissues. It promoted the growth, migration, and invasion of HCC cells, and elevated tumor growth and metastasis *in vivo* via the miR-27b-3p/NRAS axis (Lin et al., 2022). Hsa_circRNA_104348 was upregulated in HCC tissues and accelerated HCC cell growth and metastasis by the miR-187-3p/RTKN2 regulatory axis (Huang et al., 2020).

Hsa_circ_0088036 is a circRNA produced from the sushi domain containing 1 (SUSD1) gene (Dolinar et al., 2019). It was first identified as a potential blood biomarker of amyotrophic lateral sclerosis (Dolinar et al., 2019). Subsequently, researchers found that hsa_circ_0088036 was upregulated in peripheral blood mononuclear cells from patients with rheumatoid arthritis, promoting proliferation, migration, and inflammation in fibroblast-like synoviocytes in rheumatoid arthritis (Zhong et al., 2020; Geng et al., 2022). Recently, the involvement of hsa_circ_0088036 in cancers was reported. Yang et al. (2022) demonstrated that hsa_circ_0088036 was elevated in bladder cancer tissues and cell lines and that high expression of hsa_circ_0088036 was positively related to shorter overall survival and worse clinicopathological characteristics. Downregulation of hsa_circ_0088036 suppressed the growth, migration, and invasion of bladder cancer cells via miR-140-3p/FOXQ1 signaling. In non-small cell lung cancer, the upregulated expression of hsa_circ_0088036 was positively related to poor prognosis. Silencing of hsa_circ_0088036 inhibited the proliferation, invasion, migration, and epithelial-mesenchymal transition of non-small cell lung cancer cells by targeting the miR-1343-3p/Bcl-3 axis (Ge et al., 2023). However, the role of hsa_circ_0088036 in HCC remains unclear.

This study investigated the role of hsa_circ_0088036 in HCC with the hypothesis that it might contribute to tumorigenesis and oxaliplatin resistance. Hsa_circ_0088036 expression was detected in HCC tissues and cell lines. The influences of hsa_circ_0088036 on proliferation and invasion as well as chemosensitivity in HCC cells were analyzed using gain- and/or loss-of-function strategies. The mechanism of hsa_circ_0088036 in HCC was further determined. Additionally, the effects and molecular mechanisms of hsa_circ_0088036 were confirmed in a xenograft mouse model.

Materials and methods

Human sample collection

Tumor tissues and matched non-tumor samples were obtained from 62 HCC patients at our hospital between January 2021 and October 2022. Inclusion criteria were: patients diagnosed with HCC by pathological examination, no prior treatment received before surgery, and aged ≥18 years. They all signed written informed consent forms before participating. After collection, all tissues were immediately preserved at -80°C. This study was approved by the Ethics Committee of Yan'an University Xianyang Hospital (Approve No. KY2021-005).

Cell culture

The THLE-3 human normal liver epithelial cell line was purchased from the ATCC (Manassas, VA, USA) and cultured in complete BEGM medium (Lonza, Walkersville, MD, USA). Human HCC cell lines, including HepG2, Hep3B, and Huh7, were obtained from the Chinese Academy of Sciences Cell Bank (Shanghai, China) and kept in DMEM (Gibco, Grand Island, NY, USA) supplemented with 10% fetal bovine serum (FBS; Gibco). All cells were maintained in a humidified incubator with 5% CO_2 at 37°C.

Plasmid and cell transfection

Hsa_circ_0088036-overexpressing plasmid was generated using the pLC5-ciR vector (Geneseed, Guangzhou, China). To knock down hsa_circ_0088036, the hsa_circ_0088036 shRNA sequence was subcloned into the pGPU6/Neo plasmid. The hsa_circ_0088036 target sequences were : hsa_circ_0088036 shRNA-1: 5'-AACCCAGATAACAGTAAAACA-3'; hsa_circ_0088036 shRNA-2: 5'-GATAACAGTAAAACA GACCAT-3'. The pcDNA3.1-KIF2A plasmid was utilized to overexpress kinesin superfamily protein 2A (KIF2A) in HCC cells with the pcDNA3.1 empty vector as the control. miR-140-3p mimic, inhibitor, and their respective negative controls were obtained from Genepharma Co., Ltd (Shanghai, China). HepG2 and Huh7 cells were transfected with the indicated vectors using Lipofectamine™ 3000 Transfection Reagent (Invitrogen, Carlsbad, CA, USA).

CCK-8 assay

When reaching 70-80% confluency, the transfected cells were trypsinized, seeded in 96-well plates at a density of 2000 cells/well, and treated with designated concentrations of oxaliplatin, doxorubicin, or sorafenib (all from Solarbio, Beijing, China) for 48h at 37°C. Next, 10 μL CCK-8 solution (Dojindo Laboratories, Kumamoto, Japan) was added to each well and, 1h later, the optical density (OD) at 450 nm was measured using a microplate reader.

EdU proliferation assay

HepG2 and Huh7 cells (5×10^6 cells/well) were seeded in 24-well plates and cultured overnight.

Following transfection with the indicated vectors for 48h, cell proliferation was measured using an EdU assay kit (RiBoBio, Guangzhou, China) according to the manufacturer's instructions. The results were observed under a fluorescence microscope (Olympus, Tokyo, Japan) and quantified using six random fields.

Transwell invasion assay

Cell invasion was assessed using 8.0 μm Transwell plates. After transfection for 24h, cells were harvested and 5×10^4 cells were suspended in 100 μL serum-free medium and then seeded into the upper chamber containing 50 μL Matrigel-coated membrane. DMEM containing 20% FBS was added to the lower chamber. To avoid cell proliferation, cells were incubated at 37°C for 24h. The cells remaining in the upper chamber were gently cleaned off with cotton wool, and the invading cells on membranes were fixed with methanol for 10 min and stained with 0.1% crystal violet. The invading cells were photographed under a light microscope and five random fields per sample were counted.

Flow cytometry

The apoptosis of HepG2 and Huh7 cells was determined by flow cytometry using the Annexin V-FITC/propidium iodide (PI) Apoptosis kit (BD Biosciences, San Jose, CA, USA). Briefly, cells were cultured in 6-well plates and transfected with the indicated vectors. Cells were harvested 48h after transient transfection and re-suspended at 1×10^6/mL in binding buffer. The cells were then incubated with Annexin V-FITC and PI reagents for 15 min in the dark at room temperature. The apoptotic rate was measured using flow cytometry (FACScan, BD Biosciences).

Dual-luciferase reporter assay

The 3' untranslated region (UTR) of KIF2A complementary to the seed region of miR-140-3p was cloned into the pmirGLO luciferase plasmid to construct the pmirGLO-KIF2A-Wt (KIF2A-Wt) plasmid. The mutated 3'UTR of KIF2A (CAGUGUGUGUGCC AGACACCAUU) was inserted into the pmirGLO plasmid to generate the pmirGLO-KIF2A-Mut (KIF2A-Mut) plasmid. Huh7 cells were cultured in 24-well plates and co-transfected with the constructed luciferase plasmids, containing KIF2A-Wt and KIF2A-Mut, and miR-140-3p mimic or its control using Lipofectamine 3000. Firefly and Renilla luciferase activities were quantified using the dual-luciferase reporter assay system (Promega, Madison, WI, USA) 48h after transfection. The relative luciferase activity was calculated as the ratio of Firefly to Renilla luciferase activity.

Animal experiments

Six-week-old male BALB/c nude mice (n=20) were purchased from Charles River (Beijing, China). They were maintained in animal care facilities under specific pathogen-free conditions. Animal experimental procedures were approved by the Experimental Animal Care Commission of Yan'an University Xianyang Hospital (Approve No. KY2021-005). The mice were divided into four groups: sh-NC, sh-circ_0088036 (sh-1), OXA+sh-NC, and OXA+sh-circ_0088036 (OXA+sh-1) (n=5 per group). The subcutaneous part of the back of these mice was injected with 2×10^6/0.1 mL Huh7 cells stably knocked down for hsa_circ_0088036 or the control. When the tumor volume reached approximately 100 mm^3 (Mei et al., 2022), 3 mg/kg oxaliplatin was injected intraperitoneally twice weekly into the OXA+sh-NC and OXA+sh-1 groups. Mice in the sh-NC and sh-1 groups received equivalent injections of PBS. The maximum (a) and minimum diameter (b) of tumors were measured every three days after oxaliplatin injection and tumor volume (V) was calculated using the formula: $V=ab^2/2$. On day 24 after the first oxaliplatin injection, the mice were sacrificed using the cervical dislocation method. Tumors were resected for further analysis. Some tumors were immediately stored in liquid nitrogen for RNA extraction to detect hsa_circ_0088036 and miR-140-3p expression. Other parts of the tumors were fixed with 4% polyformaldehyde and embedded in paraffin. Ki-67 and KIF2A expression levels were measured using immunohistochemistry with anti-Ki-67 (1:500, Cat. #9027, Cell Signaling Technology, Danvers, MA, USA) and anti-KIF2A (1:200, Cat. ab197988, Abcam, Cambridge, MA, USA) primary antibodies.

Real-time PCR and RNase R treatment

TRIzol reagent (Invitrogen) was utilized to extract total RNA from the cells and tissues. cDNA was synthesized from 1 μg of total RNA using the SuperScriptTM One-Step Reverse Transcription Kit (Invitrogen). Gene expression was analyzed by real-time PCR with SYBR Green Master Mix (TAKARA, Japan). miR-140-3p expression was measured by the TaqMan MicroRNA Assay (Toyobo, Osaka, Japan). GAPDH (for hsa_circ_0088036, SUSD1, and KIF2A) or U6 snRNA (for miR-140-3p) was regarded as an internal reference. The $2^{-\Delta\Delta Ct}$ method was used to calculate the expression of target genes. The primers were synthesized by Sangon Biotech (Shanghai, China) and the sequences were as follows: hsa_circ_0088036 forward primer 5'-TACAATGTCAGTCTCCGGGC-3', reverse primer 5'-TGCTTCTCCATCTCAAGCAGG-3'; SUSD1 forward primer 5'- ACTTGACCACAGACAGCAGG-3', reverse primer 5'-CACTACCCAGACGGAGGTTT-3'; KIF2A forward primer 5'-AGATGAGGTGATGGCAACGG-3', reverse primer 5'-TGATGTATTCGGCCATCGCT-3'; GAPDH forward primer 5'-GAAGACGGGCGGAG AGAAAC-3', reverse primer 5'-CCCAATACGACCA AATCCGTTG-3'; miR-140-3p forward primer 5'-ACACTCCAGCTGGGUACCACAGGGUAGAA-3', reverse primer 5'-TGGTGTCGTGGAGTCG-3'; U6

forward primer 5'-TGCGGGTGCTCGCTTCGGCAGC-3', reverse primer 5'-CCAGTGCAGGGTCCGAGGT-3'.

RNase R is a strong 3' to 5' exoribonuclease that can degrade linear but not circular RNA (Suzuki and Tsukahara, 2014). For RNase R treatment, 1 μg of total RNA was incubated with 3U of RNase R (Epicenter Technologies, Madison, WI, USA) for 30 min at 37°C. The expression of hsa_circ_0088036 and SUSD1 was further analyzed by real-time PCR.

Western blot

Total proteins were extracted from tissues and cells using RIPA lysis buffer containing 1 mM PMSF. After centrifugation at 12,000 rpm for 30 min at 4°C, the supernatants were obtained to measure protein concentrations using a BCA Assay Kit (Beyotime, Shanghai, China). After mixing with 5× loading buffer, the protein samples were boiled in water to denature the proteins. Proteins (20 μg/lane) were separated by SDS-PAGE and transferred to PVDF membranes. After blocking in TBST containing 5% skim milk for 1h, the membrane was immunoblotted with primary antibodies, including anti-KIF2A (1:1000, Cat. ab197988, Abcam, Cambridge, MA, USA), anti-p-PI3K (1:1000, Cat. ab138364, Abcam), anti-p-AKT (1:2000, Cat. #4060, CST, Danvers, MA, USA), anti-Notch1 (1:1000, Cat. #3608, CST), anti-β-catenin (1:1000, Cat. #9582, CST), anti-Wnt3a (1:600, Cat. sc-136163, Santa Cruz Biotechnology, Santa Cruz, CA, USA) and anti-GAPDH (1:1000, Cat. ab9485, Abcam). Then, the membrane was incubated at room temperature with HRP-conjugated secondary antibodies for 1h. Finally, the protein bands were visualized using an ECL detection reagent (Thermo Fisher, Carlsbad, CA, USA). The results were finally quantified using the ImageJ software (National Institutes of Health). GAPDH was used as an internal control.

Table 1. The relationship between hsa_circ_0088036 expression and the clinicopathologic characteristics of HCC patients.

Parameters	Number of cases	Hsa_circ_0088036 expression		*p*-value
		Low	High	
Age (years)				0.200
<50	20	13	7	
≧50	42	20	22	
Gender				0.568
Male	53	24	29	
Female	9	5	4	
Differentiation				0.160
Well	7	5	2	
Moderately	36	13	23	
Poorly	19	6	13	
HBV infection				0.217
Negative	51	29	22	
Positive	11	4	7	
Serum AFP (ng/mL)				0.075
<20	14	9	5	
≧20	48	18	30	
Tumor size (cm)				0.003*
<5	25	17	8	
≧5	37	11	26	
Number of tumor nodules				0.301
1	47	26	21	
≧2	15	6	9	
TNM stage				0.007*
I and II	36	25	11	
III and IV	26	9	17	

HBV, hepatitis B virus; AFP, alpha-fetoprotein; TNM, tumor-node-metastasis. The "low" or "high" expression of hsa_circ_0088036 was defined according to the cut-off value (the mean value of patients). *$p<0.05$.

miRNA pull-down

Cells were grown to ~80% confluence and then transfected with 150 nM biotin-labeled miR-140-3p (Bio-miR-140-3p) or the negative control (Bio-NC), which were synthesized by GenePharma. Subsequently, cells were lysed in Pierce IP lysis buffer (25 mM Tris-HCl pH 7.4, 150 mM NaCl, 1 mM EDTA, 1% NP-40, and 5% glycerin) supplemented with protease inhibitor and RNase inhibitor, and incubated with M-280 streptavidin magnetic beads (Invitrogen) at 4°C overnight. After elution, the immunoprecipitated RNAs were extracted by Trizol and analyzed by real-time PCR.

Statistical analysis

Experimental data are expressed as the mean ± standard deviation (SD). Statistical analysis was conducted using SPSS19.0 or Graphad Prism 8 software. The difference between two groups was analyzed using the Student's t-test, and differences among three or more groups were assessed by one-way ANOVA with Tukey's *post-hoc* test. The association between hsa_circ_0088036 and patients' clinicopathological characteristics was carried out with the Chi-square test. The correlation between hsa_circ_0088036 and miR-140-3p in HCC tissues was analyzed by Pearson's correlation analysis. Differences were considered statistically significant at $p<0.05$.

Results

Hsa_circ_0088036 was highly expressed in HCC tissues and cells, with even higher expression in oxaliplatin-resistant cells

The expression of hsa_circ_0088036 was analyzed in 62 pairs of HCC and adjacent normal tissues. The results showed that, compared with adjacent normal tissues, hsa_circ_0088036 expression was dramatically increased in HCC samples (Fig. 1A). The relationship between hsa_circ_0088036 expression and the clinicopathological characteristics of HCC patients was further explored. As shown in Table 1, hsa_circ_

0088036 expression was positively correlated with tumor size and TNM stage in patients with HCC. Additionally, compared with THLE-3 human normal liver epithelial cells, hsa_circ_0088036 was highly expressed in HCC cell lines, including HepG2, Hep3B, and Huh7 (Fig. 1B). Surprisingly, hsa_circ_0088036 expression in oxaliplatin-resistant HepG2 and Huh7 cells was higher than in their parental cells (Fig. 1B). In Huh7 cells, hsa_circ_0088036 was markedly resistant to RNase R when compared with its corresponding linear transcript SUSD1 (Fig. 1C).

Hsa_circ_0088036 promoted HCC cell proliferation and invasion

Regarding the role of hsa_circ_0088036 in HCC progression, it was overexpressed in HepG2 cells and downregulated in Huh7 cells (Fig. 2A,B). As shown in Fig. 2C-E, overexpression of hsa_circ_0088036 significantly elevated the number of EdU-positive cells, whereas downregulation decreased it. Additionally, the invasive ability of HCC cells was enhanced after hsa_circ_0088036 upregulation (Fig. 2F), while knockdown notably suppressed it (Fig. 2G). These results suggested that hsa_circ_0088036 promoted HCC cell proliferation and invasion.

Knockdown of hsa_circ_0088036 enhanced chemosensitivity in HCC cells

The influence of hsa_circ_0088036 on sensitivity to oxaliplatin was analyzed in HCC cells. IC50 values of oxaliplatin were decreased in Huh7 cells after downregulation of hsa_circ_0088036 (from 4.702 to 1.885 μM) (Fig. 3A), while upregulation significantly elevated the IC50 values of oxaliplatin in HepG2 cells (from 3.87 to 11.98 μM) (Fig. 3B). Furthermore, the effect of hsa_circ_0088036 on oxaliplatin-induced apoptosis was measured by flow cytometry. As revealed in Fig. 3C,D, oxaliplatin-induced apoptosis of HCC cells was increased after downregulation of hsa_circ_0088036, whereas it was attenuated after overexpression of hsa_circ_0088036. Additionally, we also found that hsa_circ_0088036 downregulation decreased the IC50 values of doxorubicin (from 0.46 to 0.24 μg/mL) and sorafenib (from 4.07 to 2.76 μM) in Huh7 cells (Fig. 3E,F), indicating that downregulation of hsa_circ_0088036 also increased sensitivity to doxorubicin and sorafenib. These results demonstrated that the knockdown of hsa_circ_0088036 enhanced chemosensitivity in HCC cells.

Hsa_circ_0088036 negatively regulated miR-140-3p expression

Yang et al. (2022) demonstrated that hsa_circ_0088036 facilitated the progression of bladder cancer via sponging miR-140-3p. The expression of miR-140-3p was decreased in HCC tissues and cells (Gao et al., 2021). Hence, we further investigated the relationship between hsa_circ_0088036 and miR-140-3p in HCC. Upregulation of hsa_circ_0088036 downregulated miR-140-3p expression in HepG2 cells (Fig. 4A). However, hsa_circ_0088036 knockdown facilitated the expression of miR-140-3p in Huh7 cells (Fig. 4B). Then, the miRNA pull-down assay revealed that hsa_circ_0088036 was abundantly pulled down by Bio-miR-140-3p in Huh7 cells (Fig. 4C). In addition, miR-140-3p content was inversely correlated with hsa_circ_0088036 levels in human HCC samples (Fig. 4D).

KIF2A was a target of miR-140-3p

Targetscan software predicted that KIF2A was a potential target of miR-140-3p, and their binding sites are shown in Fig. 5A. Results from the dual-luciferase reporter assay confirmed that the relative luciferase activity of KIF2A-WT in the miR-140-3p mimic group was dramatically decreased when compared with the miR-NC group (Fig. 5B). Moreover, miRNA pull-down showed that KIF2A enrichment was increased in Bio-miR-140-3p when compared with its control (Fig. 5C). These results indicated that miR-140-3p could directly target KIF2A in HCC cells. The mRNA and protein levels of KIF2A were both inhibited by miR-140-3p mimic in HepG2 and Huh7 cells (Fig. 5D-F). These

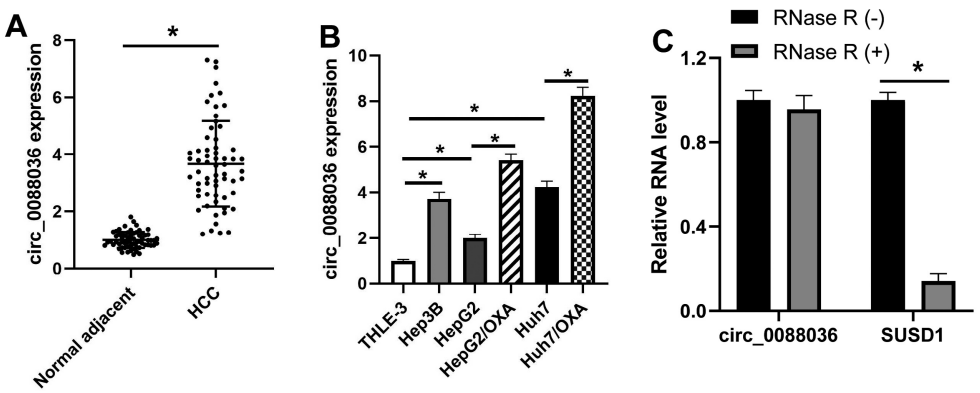

Fig. 1. Hsa_circ_0088036 expression was increased in HCC tissues and cells. **A.** Real-time PCR was used to detect hsa_circ_0088036 expression in 62 pairs of HCC tissue and adjacent normal tissues. **B.** Hsa_circ_0088036 expression in HCC cells (HepG2, Hep3B, and Huh7), oxaliplatin-resistant HepG2 and Huh7 cells, and THLE-3 human normal liver epithelial cells. **C.** Total RNA of Huh7 cells was treated with RNase R, and the mRNA expression of hsa_circ_0088036 and SUSD1 was analyzed. *$p<0.05$

results demonstrated that KIF2A was a target of miR-140-3p in HCC cells.

Hsa_circ_0088036 functioned by regulating KIF2A expression via miR-140-3p in HCC cells

Knockdown of hsa_circ_0088036 notably reduced KIF2A protein expression, which was reversed by the miR-140-3p inhibitor or KIF2A-overexpressing plasmid (Fig. 6A). Compared with the sh-hsa_circ_0088036+pcDNA3.1 group, the number of EdU-positive cells and invaded cells were both elevated in sh-hsa_circ_0088036+KIF2A group (Fig. 6B-E). Moreover, deletion of hsa_circ_0088036-induced apoptosis was attenuated after KIF2A-overexpression in oxaliplatin-exposed cells (Fig. 6F,G). Overall, hsa_circ_0088036 promoted proliferation and invasion, as well as oxaliplatin resistance, in HCC cells by positively regulating KIF2A expression through miR-140-3p.

Downregulation of hsa_circ_0088036 inhibited tumor growth and increased oxaliplatin sensitivity in vivo

The role of hsa_circ_0088036 in progression and

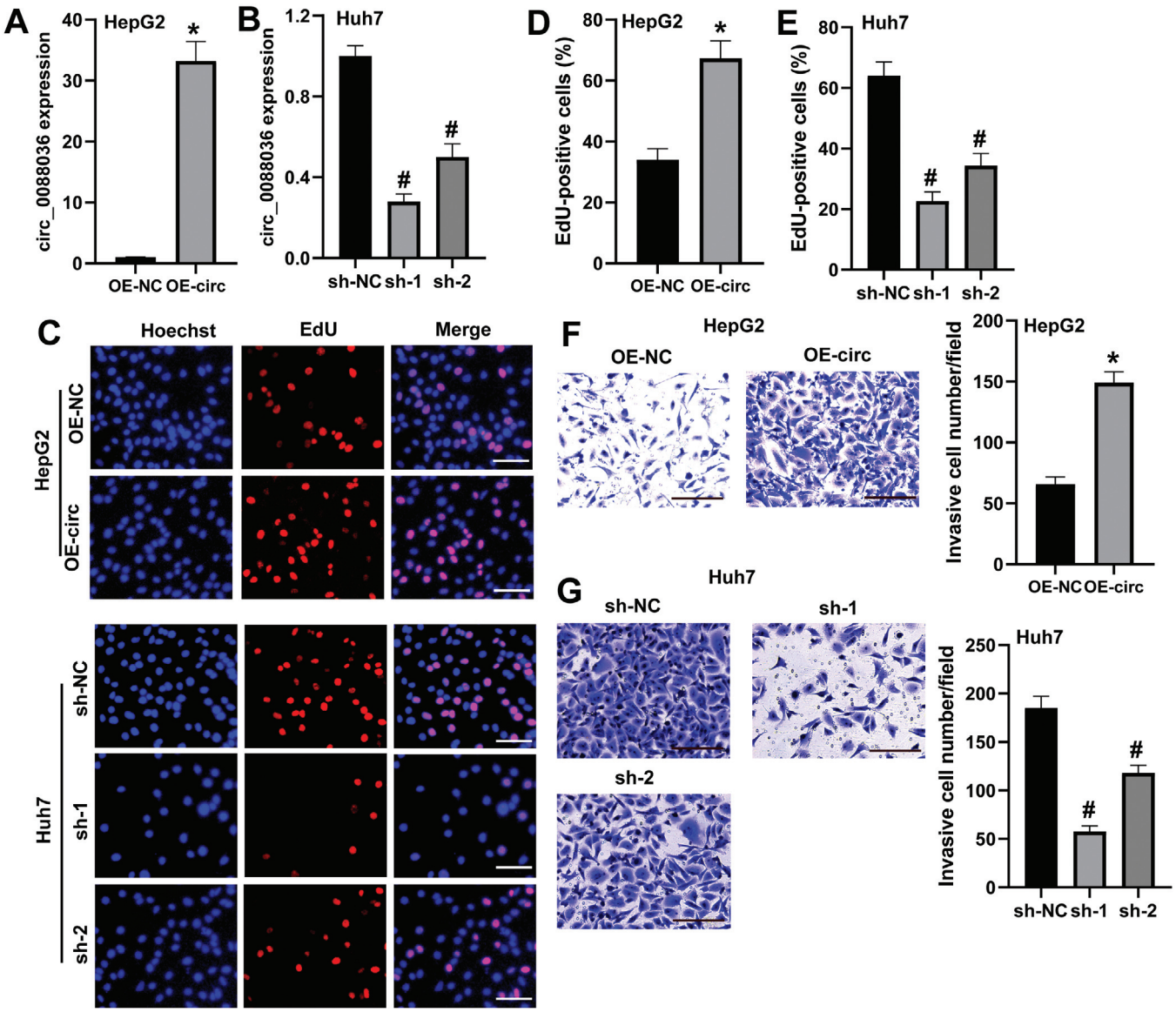

Fig. 2. Hsa_circ_0088036 promoted HCC cell proliferation and invasion. The expression of hsa_circ_0088036 in HepG2 **(A)** and Huh7 cells **(B)** was detected by real-time PCR. **C-E.** After upregulation or downregulation of hsa_circ_0088036 in HepG2 and Huh7 cells, the proliferation of cells was determined by the EdU assay, and the percentage of EdU-positive cells was measured in both cells. **F, G.** The invasion of HepG2 and Huh7 cells was analyzed by the Transwell assay *p<0.05 vs. OE-NC; $^{\#}p$<0.05 vs. sh-NC. Scale bar: C, 100 μm; F, G, 250 μm.

oxaliplatin sensitivity was further analyzed in mouse xenograft models of HCC. Hsa_circ_0088036 expression in tumor tissues was significantly inhibited in the sh-1 and OXA+sh-1 groups (Fig. 7A). Tumor volume and the expression of the proliferation biomarker Ki-67 were reduced by hsa_circ_0088036 knockdown or oxaliplatin treatment (Fig. 7B-E). Furthermore, compared with the sh-1 or OXA+sh-NC group, the combination of hsa_circ_0088036 knockdown and oxaliplatin treatment significantly suppressed tumor volumes and Ki-67 levels (Fig. 7B-E). Additionally, compared with the sh-NC group, miR-140-3p expression was increased, while KIF2A expression was decreased in tumors of the sh-1 group. Similarly, compared with the

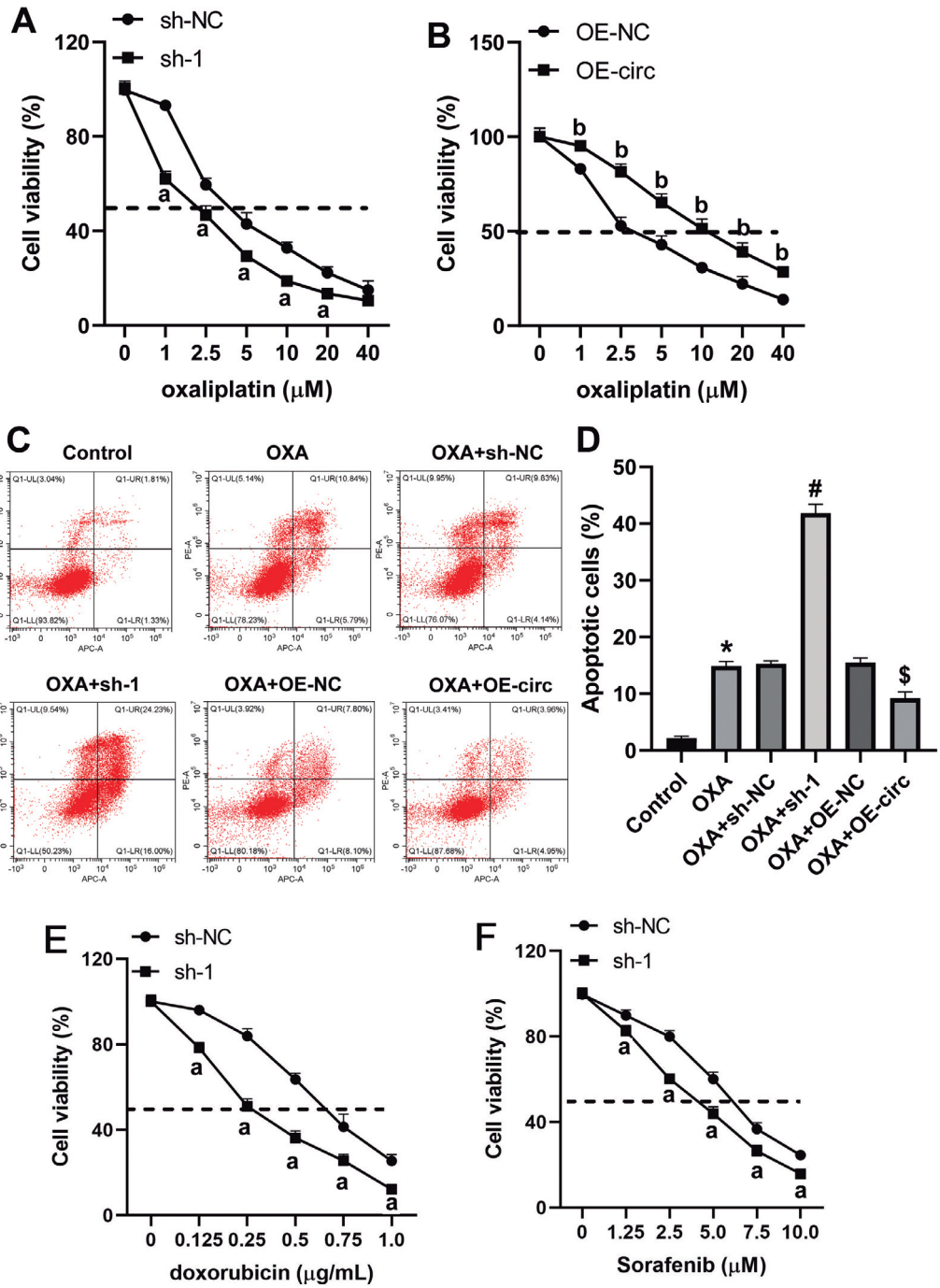

Fig. 3. Knockdown of hsa_circ_0088036 enhanced oxaliplatin sensitivity in HCC cells. **A.** Huh7 cells were transfected with hsa_circ_0088036 shRNA (sh-1) or its control sh-NC, and stimulated with different concentrations of oxaliplatin. Cell viability was detected by CCK-8, and the IC50 of each group was calculated. **B.** HepG2 cells were transfected with hsa_circ_0088036 overexpressing plasmid (OE-circ) or the OE-NC plasmid, and incubated with indicated concentrations of oxaliplatin. The IC50 of cells was measured by CCK-8. **C, D.** Huh7 cells were treated with 5 μM oxaliplatin and transfected with the designated vector, the apoptosis of cells was determined by flow cytometry and apoptotic cells were calculated. **E.** The viability of Huh7 cells transfected with sh-1 or sh-NC and treated with different concentrations of doxorubicin was examined by CCK-8. **F.** CCK-8 assay for the viability of Huh7 cells transfected with sh-1 or sh-NC and stimulated with designated concentrations of sorafenib. $^{a}p<0.05$ vs. sh-NC; $^{b}p<0.05$ vs. OE-NC; $^{*}p<0.05$ vs. Control; $^{\#}p<0.05$ vs. OXA+sh-NC; $^{\$}p<0.05$ vs. OXA+OE-NC.

OXA+sh-NC group, miR-140-3p expression was elevated, and KIF2A level was suppressed in tumors of the OXA+sh-1 group (Fig. 7D-F). These data indicated that silencing of hsa_circ_0088036 suppressed HCC cell proliferation and increased oxaliplatin sensitivity *in vivo*.

Hsa_circ_0088036/miR-140-3p/KIF2A axis regulated PI3K/Akt and Notch signaling pathways in HCC

Chen et al. (2022) used RNA-seq technology to investigate the differentially expressed genes (DEGs) in both A549 and NCI-H1975 cells after the knockdown of KIF2A, and found that DEGs were enriched in PI3K/Akt, Wnt, and Notch signaling pathways. Therefore, the effects of the hsa_circ_0088036/miR-140-3p/KIF2A axis on the activation of PI3K/Akt, Wnt/β-catenin, and Notch signaling pathways in HCC were analyzed by western blot. The results in Huh7 cells showed that downregulation of hsa_circ_0088036 notably decreased the protein levels of p-PI3K, p-Akt, and Notch1, which was reversed by the miR-140-3p inhibitor or KIF2A-overexpressing plasmid (Fig. 8A). However, the expression levels of Wnt3a and β-catenin were not changed after altering the expression of hsa_circ_0088036, miR-140-3p, and KIF2A (Fig. 8A). Moreover, after knockdown of hsa_circ_0088036, the protein levels of p-PI3K, p-Akt, and Notch1 were inhibited, and were even lower when combined with oxaliplatin in mouse tumor tissues. Downregulation of hsa_circ_0088036 did not affect the protein levels of Wnt3a and β-catenin in tumor samples (Fig. 8B). These results demonstrated that hsa_circ_0088036 activated the PI3K/Akt and Notch signaling pathways in HCC through the miR-140-3p/KIF2A axis.

Discussion

Increasing evidence has demonstrated the critical

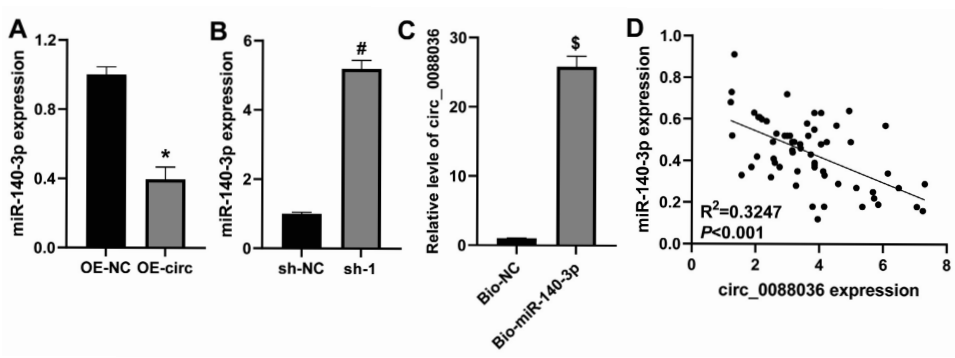

Fig. 4. Hsa_circ_0088036 negatively regulated miR-140-3p expression. **A.** HepG2 cells were transfected with hsa_circ_0088036-overexpressing plasmid (OE-circ) or control vector (OE-NC), and miR-140-3p expression was tested by real-time PCR. **B.** miR-140-3p expression was increased in Huh7 cells after hsa_circ_0088036 knockdown. **C.** miRNA pull-down assays the relationship between hsa_circ_0088036 and miR-140-3p. **D.** The correlation between hsa_circ_0088036 and miR-140-3p in human HCC tissues. *$p<0.05$ vs. OE-NC; $^{\#}p<0.05$ vs. sh-NC; $^{\$}p<0.05$ vs. Bio-NC.

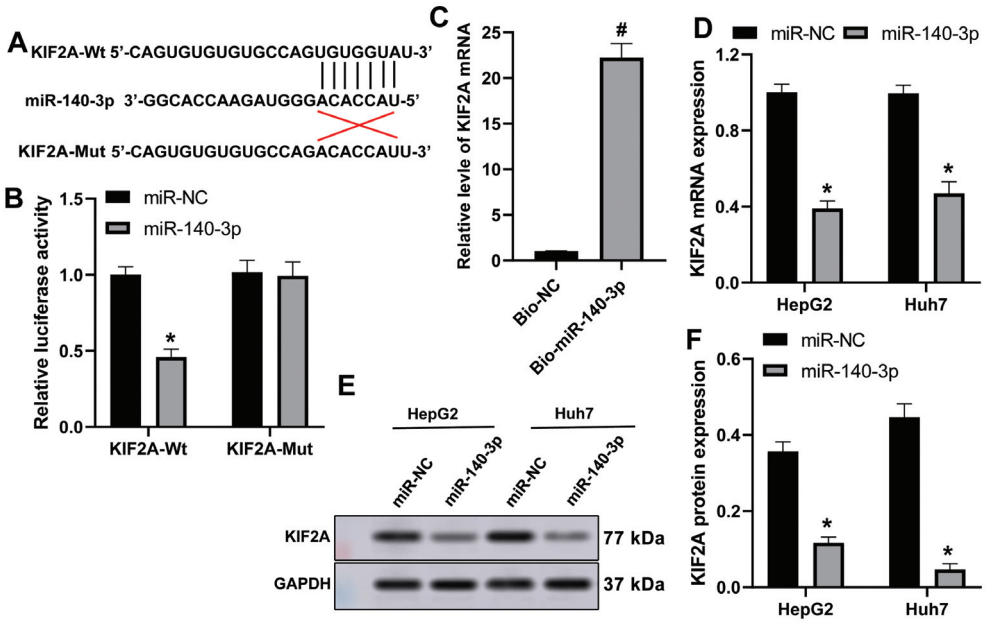

Fig. 5. KIF2A was a target of miR-140-3p in HCC. **A.** The binding sequences between KIF2A and miR-140-3p. **B.** Dual-luciferase reporter assay for the relationship between miR-140-3p and KIF2A. **C.** KIF2A enrichment was increased in Bio-miR-140-3p when compared with Bio-NC. **D.** KIF2A mRNA expression in HepG2 and Huh7 cells was measured after transfection with miR-NC or miR-140-3p mimic. **E, F.** Western blot assay for KIF2A protein levels. *$p<0.05$ vs. miR-NC; $^{\#}p<0.05$ vs. Bio-NC.

role of circRNA in human cancers. CircRNAs are not only related to proliferation and metastasis but are also involved in chemoresistance in multiple cancers. For example, circPARD3 was upregulated in laryngeal squamous cell carcinoma (LSCC) tissues. It facilitated proliferation, migration, invasion, and cisplatin resistance in LSCC cells (Gao et al., 2020). CircPTK2 significantly promoted migration, invasion, and gemcitabine resistance in bladder cancer cells as well as lymph node metastasis *in vivo* (Meng et al., 2023). In this study, we demonstrated that hsa_circ_0088036 was upregulated in HCC tumor samples. Higher expression of hsa_circ_0088036 was associated with tumor size and TNM stage in patients with HCC. This indicated that hsa_circ_0088036 might be an oncogene in HCC. Functional investigation experiments showed that upregulation of hsa_circ_0088036 promoted the proliferation and invasion of HCC cells. Contrarily, the downregulation of hsa_circ_0088036 suppressed the proliferation and invasion of HCC cells. Meanwhile, depletion of hsa_circ_0088036 inhibited tumor growth in mouse models. We also found that silencing of hsa_circ_0088036 elevated oxaliplatin sensitivity both *in vitro* and *in vivo*. These results demonstrated that hsa_circ_0088036 could promote tumorigenesis and oxaliplatin resistance in HCC cells. For the first time, our study revealed the role of hsa_circ_0088036 in HCC and it could be a novel target for HCC treatment, especially for oxaliplatin-resistant patients.

Studies have demonstrated that circRNAs play roles

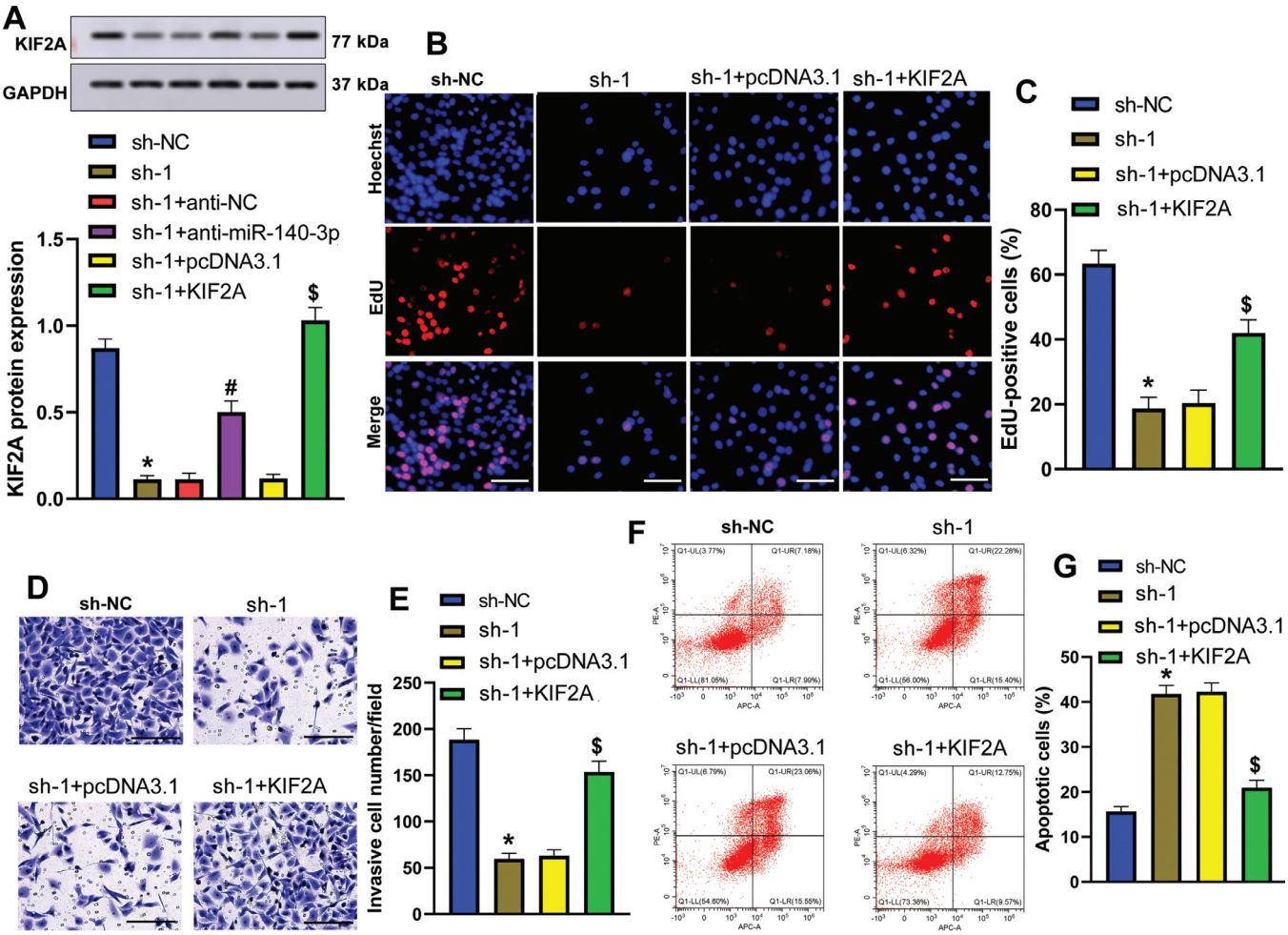

Fig. 6. Hsa_circ_0088036 functioned by regulating KIF2A expression via miR-140-3p in HCC cells. **A.** The protein expression of KIF2A in Huh7 cells under different treatments was detected by western blot. **B, C.** Huh7 cells were transfected with sh-circ_0088036 (sh-1)/sh-NC or co-transfected with sh-1 and KIF2A-overexpressing plasmid/pcDNA3.1 control, EdU was used to analyze cell proliferation. EdU-positive cells were calculated. **D, E.** The Transwell method was used to determine the invasion of Huh7 cells. **F, G.** Huh7 cells were exposed to oxaliplatin and transfected with the designated vector, and cell apoptosis was investigated by flow cytometry. $^{*}p<0.05$ vs. sh-NC; $^{\#}p<0.05$ vs. sh-1+anti-NC; $^{\$}p<0.05$ vs. sh-1+pcDNA3.1. Scale bar: B, 100 μm; D, 250 μm.

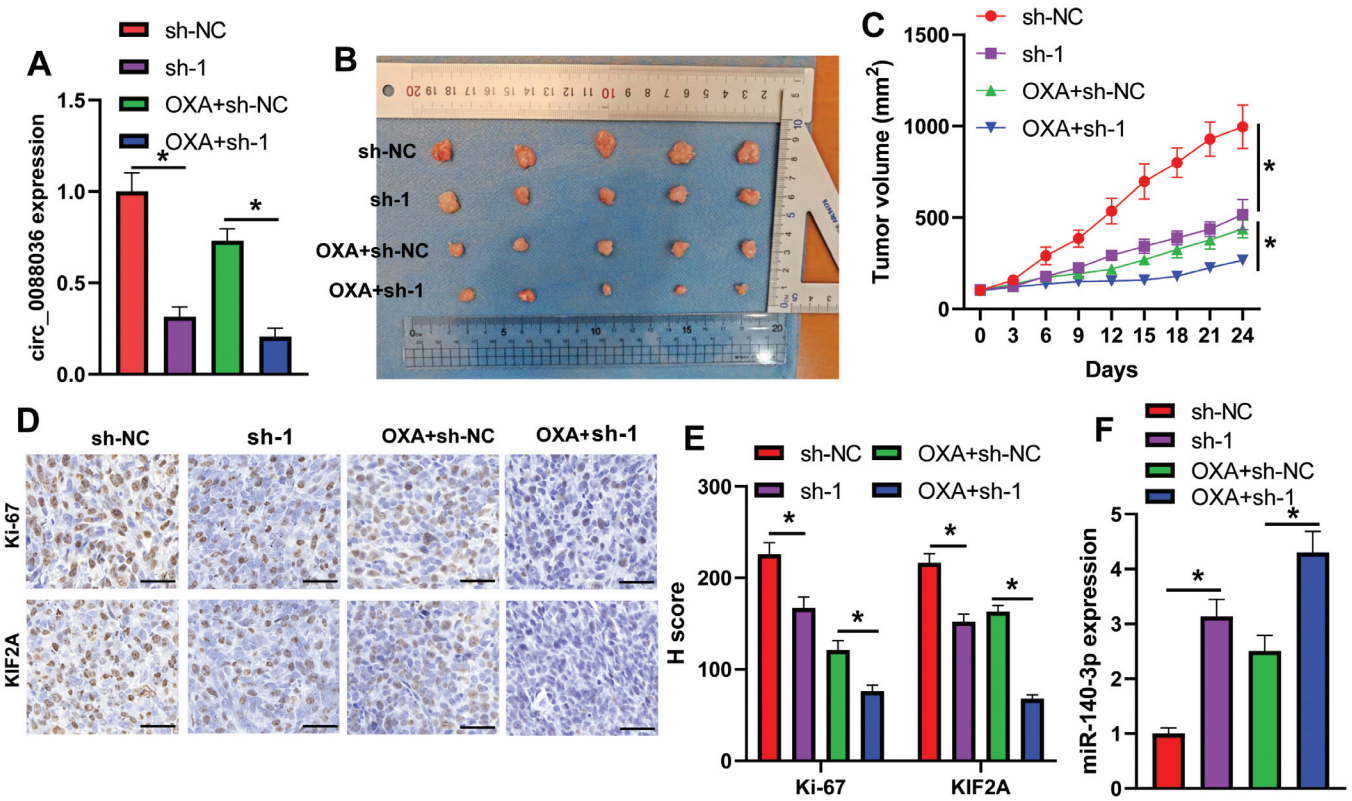

Fig. 7. Downregulation of hsa_circ_0088036 inhibited tumor growth and increased oxaliplatin sensitivity *in vivo*. **A.** The expression of hsa_circ_0088036 in tumors of mice. **B.** Representative images of tumors in different groups. **C.** Tumor volume was calculated. **D, E.** Immunohistological images of Ki-67 and KIF2A in tumor samples and semi-quantitative analyses were performed. **F.** Real-time PCR assay for miR-140-3p expression in mouse tumors. **p*<0.05. Scale bar: 50 μm.

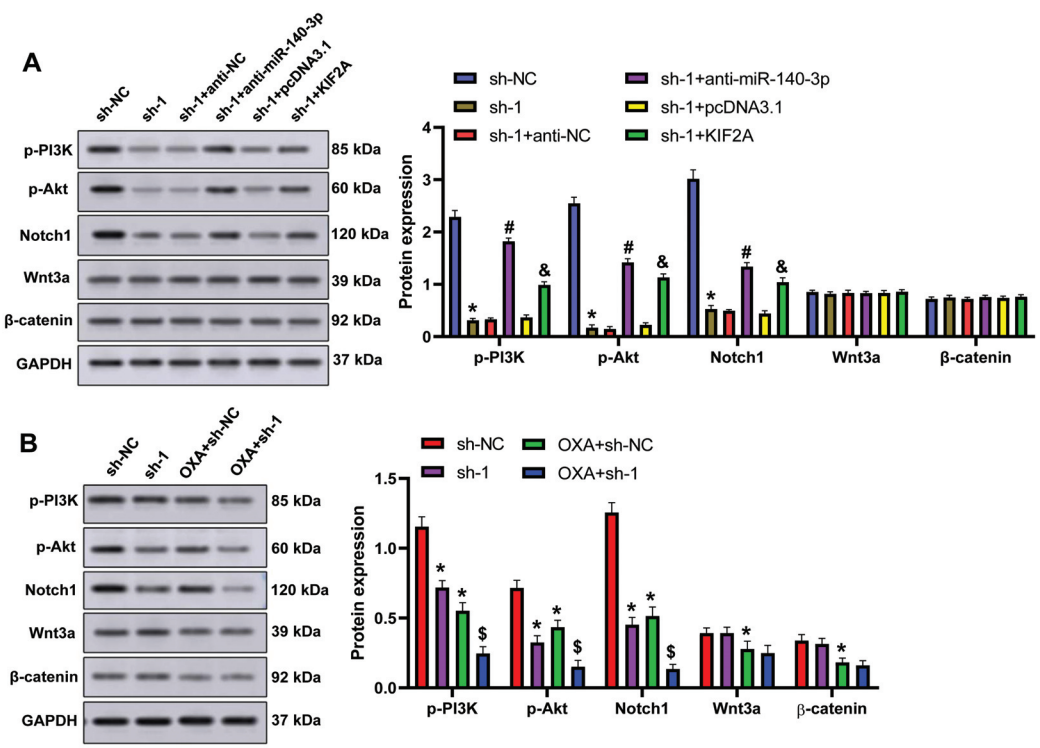

Fig. 8. Hsa_circ_0088036/miR-140-3p/KIF2A axis regulated the PI3K/Akt and Notch signaling pathways in HCC. **A.** Huh7 cells were transfected with designated vectors and the protein levels of p-PI3K, p-Akt, Notch1, Wnt3a, and β-catenin were analyzed by western blot. **B.** The protein levels of p-PI3K, p-Akt, Notch1, Wnt3a, and β-catenin in tumor tissues of mice. **p*<0.05 vs. sh-NC; #*p*<0.05 vs. sh-1+anti-NC; &*p*<0.05 vs. sh-1+pcDNA3.1; $*p*<0.05 vs. OXA+sh-NC.

in many diseases acting as miRNA sponges (Liu et al., 2019; Peng et al., 2021b). miRNAs are small and highly conserved noncoding RNAs of ~22 nucleotides in length. They typically silence target messenger RNAs (mRNAs) by binding to the 3' UTR (Haneklaus et al., 2013). Compelling evidence indicates that miRNAs have a critical effect on the pathogenesis of human diseases, especially cancers (Haneklaus et al., 2013; Xu et al., 2020; Peng et al., 2021a). They can function as tumor promotors or suppressors in different types of cancers (Peng et al., 2021a). miR-140-3p exhibits anticancer functions in many cancers, such as bladder (Wang et al., 2020), gastric (Chen et al., 2021), non-small cell lung (Hu et al., 2020), and colorectal cancer (Liu et al., 2021a). Gao et al. (Gao et al., 2021) found that miR-140-3p expression was downregulated in HCC tissues and cell lines when compared with corresponding controls. And miR-140-3p could attenuate the proliferation, migration, and invasion of HCC cells. Additionally, miR-140-3p enhanced the sensitivity of HCC cells to sorafenib (Li et al., 2018). Hsa_circ_0088036 has been shown to promote bladder cancer progression via sponging miR-140-3p (Yang et al., 2022). Therefore, we analyzed the relationship between hsa_circ_0088036 and miR-140-3p in HCC. The results showed that hsa_circ_0088036 negatively regulated miR-140-3p expression in HCC cells and xenograft mouse models. The miRNA pull-down assay confirmed the direct binding between them. Moreover, a negative correlation was observed between hsa_circ_0088036 and miR-140-3p in human HCC tissues. These data verified that hsa_circ_0088036 negatively modulated miR-140-3p expression via direct binding.

KIF2A is a member of the kinesin-13 subfamily with microtubule depolymerizing activity. It is an important regulator of the mitotic spindle (Eagleson et al., 2015). A variety of studies showed that KIF2A promoted the progression of multiple types of cancers (Wang et al., 2014; Zhang et al., 2020; Chen et al., 2022). Liu et al. (Liu et al., 2021b) found that KIF2A expression was elevated in human HCC tissues compared with adjacent tissues. KIF2A expression was involved in worse liver function, higher tumor stages, and poor overall survival in HCC patients. Also, KIF2A was more highly expressed in HCC cells than in normal human hepatocytes. Knockdown of KIF2A inhibited HCC cell proliferation, migration, and invasion via interacting with Notch1 (Wu et al., 2022). Studies have found that KIF2A could be targeted by many miRNAs, such as miR-603 (Wang et al., 2022), miR-760 (Zheng et al., 2023), miR-451a (Uchida et al., 2019), etc. Targetscan software predicted that KIF2A was a potential target of miR-140-3p. Using a dual-luciferase reporter assay and a miRNA pull-down assay, we verified that miR-140-3p could target KIF2A in HCC cells. Furthermore, we found that miR-140-3p negatively regulated KIF2A expression both at the transcriptional and translational levels. Subsequently, the relationship between hsa_circ_0088036 and KIF2A was confirmed in HCC. The results revealed that hsa_circ_0088036 knockdown notably reduced KIF2A expression both in HCC cells and *in vivo*. Overexpression of KIF2A considerably reversed the effect of hsa_circ_0088036 downregulation on proliferation, invasion, and oxaliplatin sensitivity in HCC cells. Additionally, the regulation of hsa_circ_0088036 knockdown on KIF2A expression was reversed by miR-140-3p inhibitor. These results demonstrated that hsa_circ_0088036 promoted proliferation and invasion as well as oxaliplatin resistance in HCC cells by positively regulating KIF2A expression through miR-140-3p.

Published articles have shown that KIF2A is mainly related to PI3K/Akt, Wnt/β-catenin, and Notch pathways (Xu et al., 2021; Chen et al., 2022; Wu et al., 2022; Sun et al., 2023) and these three pathways are related to chemotherapy resistance and tumor progression (Wang et al., 2010; Deldar Abad Paskeh et al., 2021; Xu et al., 2021). Therefore, we further analyzed the influence of the hsa_circ_00 88036/mR-140-3p/KIF2A axis on PI3K/Akt, Wnt/β-catenin, and Notch signaling pathways. The results revealed that the hsa_circ_00 88036/mR-140-3p/KIF2A axis could activate the PI3K/Akt and Notch signaling pathways, without any effect on Wnt/β-catenin activation in HCC.

In conclusion, this is the first study to clarify the role of hsa_circ_0088036 in HCC and KIF2A as a target of miR-140-3p. This study found that hsa_circ_0088036 promoted tumorigenesis and chemotherapy resistance in HCC via the miR-140-3p/KIF2A axis followed by the activation of PI3K/Akt and Notch signaling pathways. Targeting the hsa_circ_0088036/miR-140-3p/KIF2A axis might be a potential therapeutic strategy for chemotherapy-resistant HCC in the clinic. However, this study has some limitations. Firstly, the role and mechanism of hsa_circ_0088036 on HCC metastasis have not been investigated *in vivo*. Secondly, the relationships between hsa_circ_0088036 and prognosis as well as chemotherapy treatment of HCC patients have not yet been analyzed. Thirdly, the use of cell lines may not fully represent the complexities of the tumor microenvironment in human patients. Further research is needed to address the limitations mentioned above.

Funding. This study was supported by the Key R&D Program of Xianyang City (No. L2022ZDYFSF078).

Conflict of interest. The authors have no relevant financial or non-financial interests to disclose.

Author's Contribution. Zhong Wang and Wen Chang designed this study. Zhong Wang, Lei Wang, Guoqing Yin, and Rong Zhang performed the experiments. Heng Li and Yuan Feng collected and analyzed the data. Zhong Wang prepared the original manuscript. All authors reviewed the manuscript.

Data Availability. The datasets generated during and/or analyzed during the current study are available from the corresponding author upon reasonable request.

References

Chen J., Cai S., Gu T., Song F., Xue Y. and Sun D. (2021). MiR-140-3p impedes gastric cancer progression and metastasis by regulating BCL2/BECN1-mediated autophagy. Onco. Targets Ther. 14, 2879-2892.

Chen J., Wen J., Liu D., Xu X., Fan M. and Zhang Z. (2022). The molecular mechanism of kinesin family member 2A (KIF2A) underlying non-small cell lung cancer: the effect of its knockdown on malignant behaviors, stemness, chemosensitivity, and potential regulated signaling pathways. Am. J. Transl. Res. 14, 68-85.

Deldar Abad Paskeh M., Mirzaei S., Ashrafizadeh M., Zarrabi A. and Sethi G. (2021). Wnt/β-Catenin signaling as a driver of hepatocellular carcinoma progression: an emphasis on molecular pathways. J. Hepatocell. Carcinoma 8, 1415-1444.

Dolinar A., Koritnik B., Glavac D. and Ravnik-Glavac M. (2019). Circular RNAs as potential blood biomarkers in amyotrophic lateral sclerosis. Mol. Neurobiol. 56, 8052-8062.

Eagleson G., Pfister K., Knowlton A.L., Skoglund P., Keller R. and Stukenberg P.T. (2015). Kif2a depletion generates chromosome segregation and pole coalescence defects in animal caps and inhibits gastrulation of the Xenopus embryo. Mol. Biol. Cell 26, 924-937.

Gao W., Guo H., Niu M., Zheng X., Zhang Y., Xue X., Bo Y., Guan X., Li Z., Guo Y., He L., Zhang Y., Li L., Cao J. and Wu Y. (2020). CircPARD3 drives malignant progression and chemoresistance of laryngeal squamous cell carcinoma by inhibiting autophagy through the PRKCI-Akt-mTOR pathway. Mol. Cancer 19, 166.

Gao C., Wen Y., Jiang F., Gu X. and Zhu X. (2021). Circular RNA circ_0008274 upregulates granulin to promote the progression of hepatocellular carcinoma via sponging microRNA-140-3p. Bioengineered 12, 1890-1901.

Ge P., Chen X., Liu J., Jing R., Zhang X. and Li H. (2023). Hsa_circ_0088036 promotes nonsmall cell lung cancer progression by regulating miR-1343-3p/Bcl-3 axis through TGFbeta/Smad3/EMT signaling. Mol. Carcinog. 62, 1073-1085.

Geng X., Zhao C., Zhang Z., Liu Y., Zhang X. and Ding P. (2022). Circ_0088036 facilitates the proliferation and inflammation and inhibits the apoptosis of fibroblast-like synoviocytes through targeting miR-326/FZD4 axis in rheumatoid arthritis. Autoimmunity 55, 157-167.

Haneklaus M., Gerlic M., O'Neill L.A. and Masters S.L. (2013). miR-223: Infection, inflammation and cancer. J. Intern. Med. 274, 215-226.

Hou Z., Liu J., Jin Z., Qiu G., Xie Q., Mi S. and Huang J. (2022). Use of chemotherapy to treat hepatocellular carcinoma. Biosci. Trends 16, 31-45.

Hu C., Zou Y. and Jing L.L. (2020). miR-140-3p inhibits progression of non-small cell lung cancer by targeting Janus kinase 1. J. Biosci. 45, 48.

Huang G., Liang M., Liu H., Huang J., Li P., Wang C., Zhang Y., Lin Y. and Jiang X. (2020). CircRNA hsa_circRNA_104348 promotes hepatocellular carcinoma progression through modulating miR-187-3p/RTKN2 axis and activating Wnt/β-catenin pathway. Cell Death Dis. 11, 1065.

Li J., Zhao J., Wang H., Li X., Liu A., Qin Q. and Li B. (2018). MicroRNA-140-3p enhances the sensitivity of hepatocellular carcinoma cells to sorafenib by targeting pregnenolone X receptor. Onco. Targets Ther. 11, 5885-5894.

Lin X.H., Liu Z.Y., Zhang D.Y., Zhang S., Tang W.Q., Li D.P., Zhang F., Chen R.X., Weng S.Q., Xue R.Y. and Dong L. (2022). circRanGAP1/miR-27b-3p/NRAS Axis may promote the progression of hepatocellular Carcinoma. Exp. Hematol. Oncol. 11, 92.

Liu Z., Zhou Y., Liang G., Ling Y., Tan W., Tan L., Andrews R., Zhong W., Zhang X., Song E. and Gong C. (2019). Circular RNA hsa_circ_001783 regulates breast cancer progression via sponging miR-200c-3p. Cell Death Dis. 10, 55.

Liu D., Chen C., Cui M. and Zhang H. (2021a). miR-140-3p inhibits colorectal cancer progression and its liver metastasis by targeting BCL9 and BCL2. Cancer Med. 10, 3358-3372.

Liu W., Xu C., Meng Q. and Kang P. (2021b). The clinical value of kinesin superfamily protein 2A in hepatocellular carcinoma. Clin. Res. Hepatol. Gastroenterol. 45, 101527.

Llovet J.M., Kelley R.K., Villanueva A., Singal A.G., Pikarsky E., Roayaie S., Lencioni R., Koike K., Zucman-Rossi J. and Finn R.S. (2021). Hepatocellular carcinoma. Nat. Rev. Dis. Primers 7, 6.

Mei J., Lin W., Li S., Tang Y., Ye Z., Lu L., Wen Y., Kan A., Zou J., Yu C., Wei W. and Guo R. (2022). Long noncoding RNA TINCR facilitates hepatocellular carcinoma progression and dampens chemosensitivity to oxaliplatin by regulating the miR-195-3p/ST6GAL1/NF-κB pathway. J. Exp. Clin. Cancer Res. 41, 5.

Meng X., Xiao W., Sun J., Li W., Yuan H., Yu T., Zhang X. and Dong W. (2023). CircPTK2/PABPC1/SETDB1 axis promotes EMT-mediated tumor metastasis and gemcitabine resistance in bladder cancer. Cancer Lett. 554, 216023.

Peng B., Theng P.Y. and Le M.T.N. (2021a). Essential functions of miR-125b in cancer. Cell Prolif. 54, e12913.

Peng F., Gong W., Li S., Yin B., Zhao C., Liu W., Chen X., Luo C., Huang Q., Chen T., Sun L., Fang S., Zhou W., Li Z. and Long H. (2021b). CircRNA_010383 acts as a sponge for miR-135a, and its downregulated expression contributes to renal fibrosis in diabetic nephropathy. Diabetes 70, 603-615.

Shen Y., Zhang N., Chai J., Wang T., Ma C., Han L. and Yang M. (2023). CircPDIA4 induces gastric cancer progression by promoting ERK1/2 activation and enhancing biogenesis of oncogenic circRNAs. Cancer Res. 83, 538-552.

Shi Y., Niu Y., Yuan Y., Li K., Zhong C., Qiu Z., Li K., Lin Z., Yang Z., Zuo D., Qiu J., He W., Wang C., Liao Y., Wang G., Yuan Y. and Li B. (2023). PRMT3-mediated arginine methylation of IGF2BP1 promotes oxaliplatin resistance in liver cancer. Nat. Commun. 14, 1932.

Sun M., Wang L., Ge L., Xu D. and Zhang R. (2023). IGF2BP1 facilitates non-small cell lung cancer progression by regulating the KIF2A-mediated Wnt/β-catenin pathway. Funct. Integr. Genomics 24, 4.

Sung H., Ferlay J., Siegel R.L., Laversanne M., Soerjomataram I., Jemal A. and Bray F. (2021). Global Cancer Statistics 2020: GLOBOCAN Estimates of Incidence and Mortality Worldwide for 36 Cancers in 185 Countries. CA. Cancer J. Clin. 71, 209-249.

Suzuki H. and Tsukahara T. (2014). A view of pre-mRNA splicing from RNase R resistant RNAs. Int. J. Mol. Sci. 15, 9331-9342.

Uchida A., Seki N., Mizuno K., Yamada Y., Misono S., Sanada H., Kikkawa N., Kumamoto T., Suetsugu T. and Inoue H. (2019). Regulation of *KIF2A* by antitumor *miR-451a* inhibits cancer cell aggressiveness features in lung squamous cell carcinoma. Cancers 11, 258.

Vogel A., Meyer T., Sapisochin G., Salem R. and Saborowski A. (2022). Hepatocellular carcinoma. Lancet 400, 1345-1362.

Wang Z., Li Y., Ahmad A., Azmi A.S., Banerjee S., Kong D. and Sarkar

F.H. (2010). Targeting Notch signaling pathway to overcome drug resistance for cancer therapy. Biochim. Biophys. Acta 1806, 258-267.

Wang J., Ma S., Ma R., Qu X., Liu W., Lv C., Zhao S. and Gong Y. (2014). KIF2A silencing inhibits the proliferation and migration of breast cancer cells and correlates with unfavorable prognosis in breast cancer. BMC Cancer 14, 461.

Wang Y., Chen J., Wang X. and Wang K. (2020). miR-140-3p inhibits bladder cancer cell proliferation and invasion by targeting FOXQ1. Aging 12, 20366-20379.

Wang F., Li J., Li L., Chen Z., Wang N., Zhu M., Mi H., Xiong Y., Guo G. and Gu Y. (2022). Circular RNA circ_IRAK3 contributes to tumor growth through upregulating KIF2A via adsorbing miR-603 in breast cancer. Cancer Cell Int. 22, 81.

Wu Q., Ren X., Chen Y., Jin Y., Zhan X., Liu C. and Zhang B. (2022). KIF2A participates in the progression of hepatocellular carcinoma and angiogenesis by interacting with Notch1. Exp. Ther. Med. 24, 683.

Xu W., Hua Y., Deng F., Wang D., Wu Y., Zhang W. and Tang J. (2020). MiR-145 in cancer therapy resistance and sensitivity: A comprehensive review. Cancer Sci. 111, 3122-3131.

Xu L., Zhang X., Wang Z., Zhao X., Zhao L. and Hu Y. (2021). Kinesin family member 2A promotes cancer cell viability, mobility, stemness, and chemoresistance to cisplatin by activating the PI3K/AKT/VEGF signaling pathway in non-small cell lung cancer. Am. J. Transl. Res. 13, 2060-2076.

Xue C., Li G., Zheng Q., Gu X., Bao Z., Lu J. and Li L. (2022). The functional roles of the circRNA/Wnt axis in cancer. Mol. Cancer 21, 108.

Yang J., Qi M., Fei X., Wang X. and Wang K. (2022). Hsa_circRNA_0088036 acts as a ceRNA to promote bladder cancer progression by sponging miR-140-3p. Cell Death Dis. 13, 322.

Yu N., Gong H., Chen W. and Peng W. (2023). CircRNA ZKSCAN1 promotes lung adenocarcinoma progression by miR-185-5p/TAGLN2 axis. Thorac. Cancer 14, 1467-1476.

Zhang X., Wang Y., Liu X., Zhao A., Yang Z., Kong F., Sun L., Yu Y. and Jiang L. (2020). KIF2A promotes the progression via AKT signaling pathway and is upregulated by transcription factor ETV4 in human gastric cancer. Biomed. Pharmacother. 125, 109840.

Zheng P., Jiang J., Li L., Wei L., Li J. and Jin L. (2023). Circ_SATB2 knockdown inhibits the tumorigenesis of non-small cell lung cancer via miR-760/KIF2A axis. Histol. Histopathol. 38, 431-441.

Zhong S., Ouyang Q., Zhu D., Huang Q., Zhao J., Fan M., Cai Y. and Yang M. (2020). Hsa_circ_0088036 promotes the proliferation and migration of fibroblast-like synoviocytes by sponging miR-140-3p and upregulating SIRT 1 expression in rheumatoid arthritis. Mol. Immunol. 125, 131-139.

Zhu G., Chang X., Kang Y., Zhao X., Tang X., Ma C. and Fu S. (2021). CircRNA: A novel potential strategy to treat thyroid cancer (Review). Int. J. Mol. Med. 48, 201.

Accepted November 19, 2024